First principles study of the stability and diffusion mechanism of a carbon vacancy in the vicinity of a SiO_2/4H-SiC interface

Hind Alsnani*, [1], J. P. Goss [1], P. R. Briddon [1], M. J. Rayson [1], A. B. Horsfall [2]

[1] School of Engineering, Newcastle University, Newcastle upon Tyne NE1 7RU, UK
[2] Department of Engineering, Durham University, Durham, DH1 3LE, UK.

Key words: DFT; diffusion; 4H-SiC ; interface

*Corresponding author: e-mail h.a.t.alsnani2@ncl.ac.uk

We have studied the carbon vacancy in bulk 4H-SiC and in the vicinity of an SiO /(0001)-4H-SiC interface using density functional theory. We find that migration is hindered in the immediate vicinity of the interface, with the energy barrier for diffusion being approximately 15% greater than the same defect in bulk 4H-SiC. In this paper we show the increased barrier is a consequence of the stabilisation of the vacancy in the immediate interface due to a combination of strengthened reconstructions and interfacial relaxation, coupled with a destabilisation of the transition state structure.

1 Introduction

Experimentally, accurate and reproducible control of the concentration of deep-level defects within the active region of SiC devices is a significant challenge. 4H-SiC is attractive for the realisation of high-power, high-temperature electronics due to its relatively wide band-gap (3.23 eV), which corresponds [1] to an intrinsic temperature of close to 1000 $^\circ$C. Furthermore, SiC has the advantage of having silicon dioxide (SiO_2) as its native oxide, a clear benefit to the use of SiC in electronic devices. However, SiC also has the potential for an array of impurities and native defects [1, 2] distinguished by composition, orientation and site within the crystal structure; a major impediment to the exploitation of SiC in electronics is the fact that the majority of common-point defects present from growth and processing, including oxidation, are electrically active with trap-levels deep within the bandgap. Arguably the biggest challenge to the realisation of SiC devices is in obtaining a high power-density, for which the problem of a high density of interface states resulting in poor surface electron mobility must be resolved. Effective mobility is significantly reduced by interface states and Coulomb scattering with a large number of traps becoming filled during inversion, causing Coulomb scattering of mobile charges.

A number of computational studies have investigated the mechanism of defect generation during oxidation at SiO_2/(0001)-4H-SiC interfaces. Although studies have been performed

relating to defects as a function of distance from a SiO_2 interface, such as oxygen-related centres [3], to our knowledge the investigations associated with carbon vacancies in this environment are rather limited. Carbon vacancies (V_C) have received particular attention due to the idea that processing SiC for devices produces these defects, which are subsequently difficult to remove. Deep electron and hole traps degrade carrier transport properties, especially in terms of leading to a lower electron mobility than required for efficient devices. Understanding their energetics is therefore very important. Centres labelled $Z_{1/2}$ and $EH_{6/7}$ are the most common deep levels observed in as-grown n-type 4H-SiC [4], for which there is evidence linking the traps to carbon vacancies in the material, incorporated as a consequence of the growth conditions. For example, there is a reduction in the concentration of $Z_{1/2}$ after C^+ implantation or thermal oxidation, both of which are known to create carbon interstitials within SiC [2, 5], which annihilate with the carbon vacancies. There is also theoretical support for this assignment [6].

The motivation of our theoretical studies is to understand the dynamics of V_C in terms of the energetics of diffusion processes in the vicinity of a SiO_2/(0001)-4H-SiC interface, based upon density functional theory simulations as encoded in the AIMPRO software package [7]. We have previously reported [8] that diffusion at the SiO_2/(0001)-4H-SiC interface is hindered, with the overall activation energy being around 0.5 eV (15%) higher than the corresponding migration barrier of this native defect in bulk 4H-SiC. Here, we focus upon the details of the geometry and electronic structure of the vacancy as it moves in the interfacial layer. The physical origins of the dependence of the activation energy upon proximity to the SiO_2/4H-SiC interface will be explained in terms of stabilisation of the vacancy in the immediate interface and an increase in the transition state energy. This calculated hindering of the diffusion is in line with the experimental observation [2] of an enhanced stability of the vacancy in such interfaces during annealing.

2 Computational method

We have performed density-functional theory (DFT) simulations within the local-density approximation [9], as implemented in the *ab initio* modelling program (AIMPRO)[7]. Electron wave functions are expanded in independent sets of s-, p- and d-Gaussian orbitals of 28 function per atom to represent Si and C [10]. Where hydrogen is included to eliminate surface dangling-bonds, it is modelled using three sets of independent s- and p-Gaussian functions, amounting to 12-functions per H atom, and oxygen in the SiO_2 layer are treated with s-, p- and d-Gaussian orbitals of four widths, amounting to 40 functions per atom. A plane-wave expansion of density and Kohn-Sham potential [12] was used to determine the matrix elements of the Hamiltonian, with a cut off of 175 Ha, yielding well-converged total energies.

The Brillouin zone of bulk 4H-SiC is sampled with a grid of $6\times6\times2$ k-points within the Monkhorst-Pack scheme [13] for the primitive cell, with similar sampling densities adopted for non-primitive supercells. This sampling density yields a total energy converged to within 10^{-5} Ha/atom.

Structural optimisation is performed using a conjugate gradients scheme, with final forces being required to be less than 10^{-3} au, and the final structural optimisation step is required to reduce the total energy by less than 10^{-5} Ha. The calculated lattice-constants of 4H-SiC are

$a_0 = 3.06$ Å and $c = 10.04$ Å, in good agreement with the literature [16, 21].

The model SiO_2/(0001)-4H-SiC system used for this study is comprised from SiO_2 on top of the k-site Si-face of 4H-SiC[22, 23]. Slabs comprised from 4H-SiC and SiO_2 are separated by vacuum in the [0001]-direction, with surface dangling bonds passivated by hydrogen, as shown in Fig. 1. Each Si and C layer in the slab are comprised from 16 atoms, so that the in-plane separation is more than 1 nm. Control calculations have been performed using bulk 4H-SiC supercells comparable to the SiC section of the slab model.

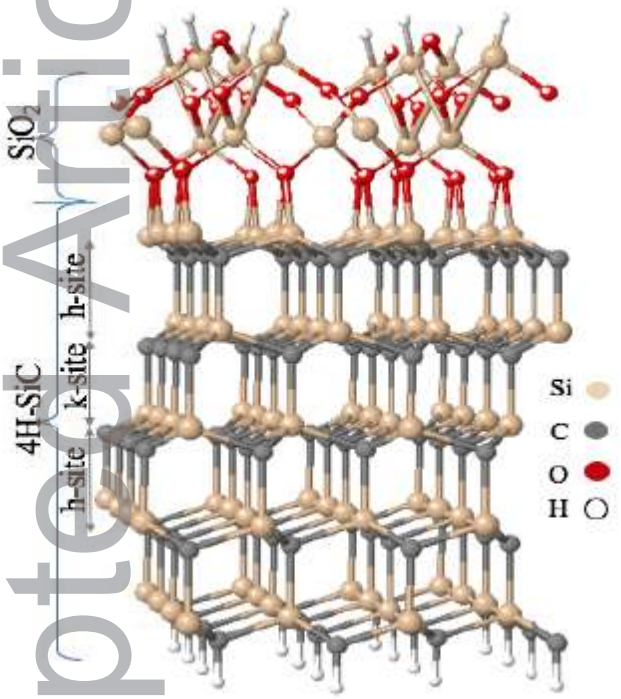

Figure 1: Schematic illustrations of SiO_2/(0001)-4H-SiC used for this stud.

Vacancies in the three C-layers increasingly distant from the interface are denoted V_C^1, V_C^2 and V_C^3. For this study layers 1 and 3 are h-site and layer 2 is k-site. We denote fully relaxed bulk vacancies as V_C^h and V_C^k, and V_C^{h*} denotes the trivial model of the vacancy formed by removal of a C atom without subsequent optimisation.

Diffusion barriers and reaction pathways of defects in bulk 4H-SiC and at interface, are obtained using the climbing nudged elastic band algorithm (cNEB) [14], with seven images.

3 Results and discussions

We first outline the case in pure SiC.

3.1 V_C in bulk 4H-SiC

There are two non-equivalent forms of carbon vacancy in 4H-SiC: the k-site (V_C^k) and the h-site (V_C^h). Optimised V_C for these sites were obtained for bulk SiC and the results used as control data for V_C in the vicinity of the interface. Figure 2 illustrates schematically the structures showing the four nearest silicon neighbours of the vacated site; sites labelled 1–3 are in a common basal-plane and site 4 is along the c-axis relative to the vacant site.

In the neutral charge state V_C forms two reconstructed Si–Si covalent bonds, resulting in pairs of the silicon atoms closer to each other than is the case in pure 4H-SiC. Deviations from the bulk Si-Si separation (d_1 and d_2 in Fig. 2) are listed in Table 1. The Si-Si reconstructed bond-lengths in bulk 4H-SiC are found to be around 10% shorter for both the h- and k-site, in good agreement with the earlier calculations [15]. In addition to the reconstructions at the h and k sites being very similar in magnitude, examination of the resulting gap-state orbitals indicates that they are qualitatively the same in localisation.

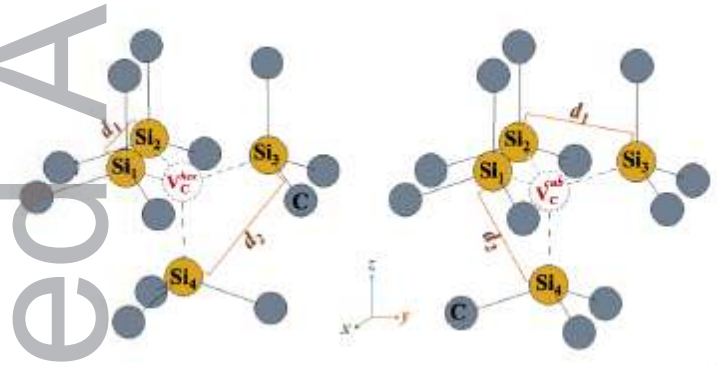

Figure 2: Schematic atomic structure indicating the local arrangement of atoms in the vicinity of V_C labelling the two reconstructed bonds of length d_1 and d_2. Si and C atoms are shown in yellow and grey, respectively.

Table 1: Deviations (Å) of the bond-lengths of the reconstructions in V_C in bulk 4H-SiC and in the vicinity of a SiO_2/(0001)-4H-SiC interface (Fig. 2) relative to the Si-Si distance in pure 4H-SiC (3.05–3.06Å within our computational approach). V_C^i indicate the vacancies in the i^{th} layer (odd layers are h-site and even k-site). Values in parentheses indicate the reduction in distance as a percentage of the pure 4H-SiC reference distance.

Position	Δd_1	Δd_2
V_C^h	0.31 (10)	0.29 (9)
V_C^1	0.35 (11)	0.39 (13)

V_C^3	0.31 (10)	0.30 (10)
V_C^k	0.29 (9)	0.38 (12)
V_C^2	0.24 (8)	0.37 (12)

A carbon vacancy is understood to move through the SiC lattice by direct exchange with an atom of the same type from an adjacent site of the same species. There are multiple diffusions pathway by which the vacancy might move, depending upon whether the vacancy is V_C^k or V_C^h at the beginning and end of the process, with basal-plane diffusion being $k \leftrightarrow k$ and $h \leftrightarrow h$, and diffusion along the c-axis being $h \leftrightarrow k$. These basic processes are labelled hh, kk and hk for brevity. The calculated migration barriers for V_C in the neutral charge state are 3.3 eV, 3.4 eV, 3.9 eV and 3.9 eV for hh, kk, hk and kh, respectively [8].

3.2 V_C at the SiO_2/(0001)-4H-SiC interface

Of initial note, the magnitude of the diffusion barrier in the interface is found to be higher than for the comparable bulk process (Fig. 3). A higher barrier can arise from changes in energy of (i) the saddle-point, (ii) the equilibrium structures, or (iii) a combination of (i) and (ii). In order to fully resolve the origin of the increased barrier in the immediate vicinity of the SiO_2/SiC interface, the diffusion energy profiles must be placed on a common energy scale. One should note that the barriers calculated using the interfacial slab are very slightly dependent upon the pairs of sites between which the diffusion takes place due to the symmetry lowering effect of the SiO_2. However, different processes within a single layer are found to differ by the order of 10 meV or less. We have set the zero on the energy scale to be that of V_C^h in the bulk-region of the slab model.

Fig. 3 shows the diffusion energy profiles between neighbouring sites in a basal plane for the first three layers of the interface slab (dotted red lines) in comparison to those for bulk 4H-SiC (solid blue lines). The data show that for the hh process the saddle point energy in the interface-layer is higher than the corresponding case in bulk, whereas the equilibrium structures are lower. Thus, we find that the interface with SiO_2 stabilises the vacancy in its equilibrium form and destabilises it at the transition state.

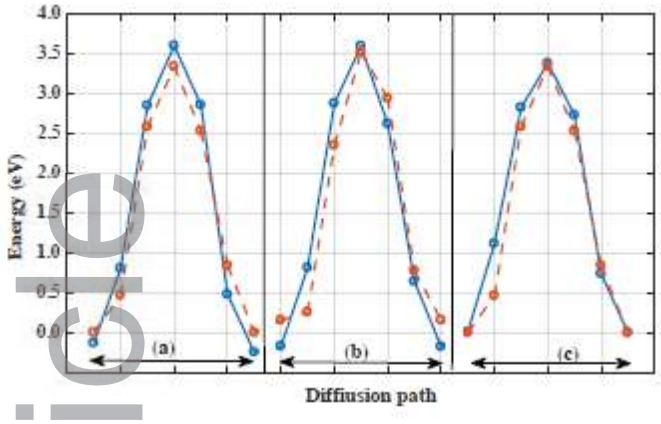

Figure 3: Minimum energy path energy profiles for three layers adjacent to the SiO_2/SiC interface (solid blue lines): (a) and (c) show *hh*-process (V_C^1 and V_C^3), and (b) shows the *kk*-process (V_C^2). In each case the underlying red dashes show the energy profile for bulk 4H-SiC. The energy scale is set to zero for V_C^h. Symbols show the energies obtained using the NEB method, with the lines joining them a guide to the eye.

The origin of the impact upon the energies as a function of distance from the interface has been explored for this study. We start with the explanation for the stabilisation of the vacancy in the interface layer.

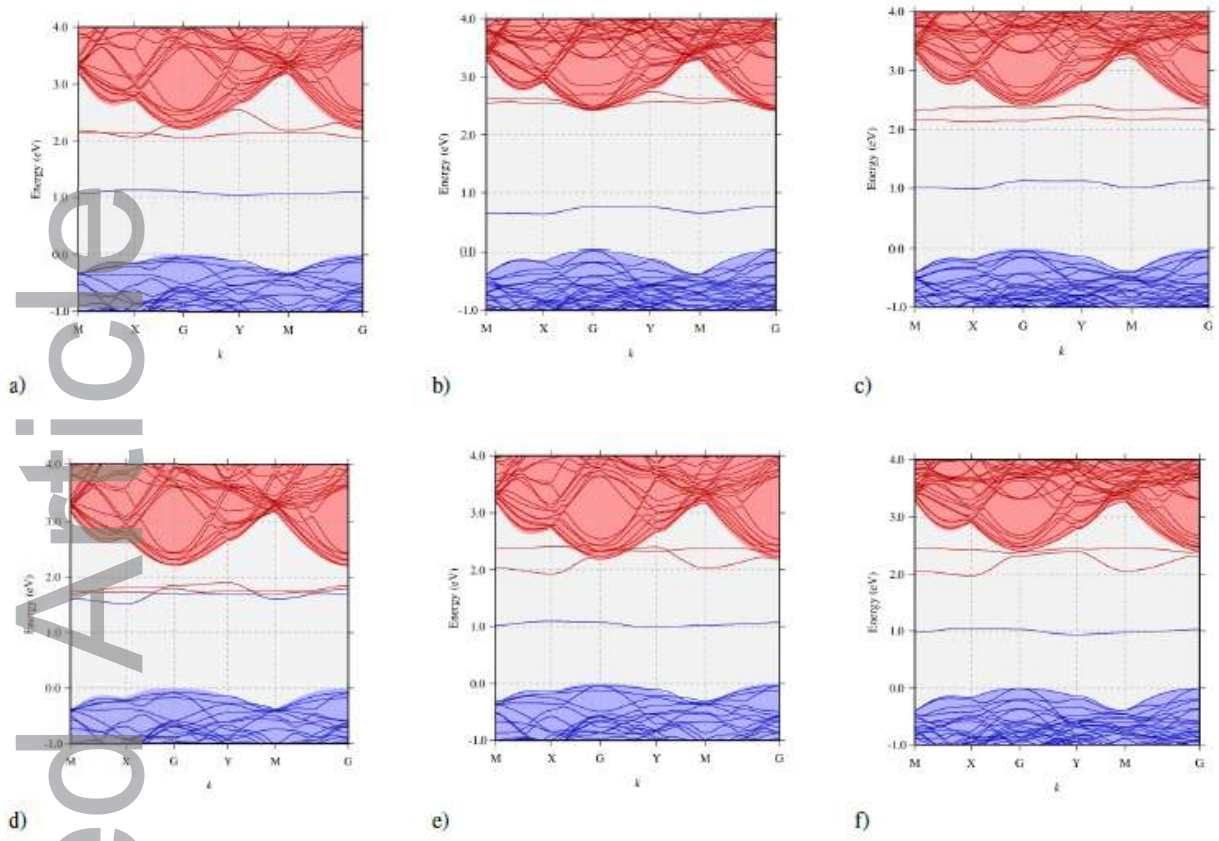

Figure 4: Electronic band structures of V_C bulk 4H-SiC and at three sites in the SiO_2/4H-SiC interface slab: a) V_C^h, b) V_C^1, c) V_C^3, d) V_C^{h*}, e) V_C^k and f) V_C^2. Occupied and unoccupied states are depicted as solid blue and red lines respectively, with the envelope of the band-structure for the underlying shaded regions show the electronic band structure for the corresponding bulk 4H-SiC supercell (128-atoms) and interface (268-atoms). The energy scale is defined such that the valence band maxima are at zero. Only states in the region of the band-gap are plotted. The k-axis labels show the high symmetry zone-centre (G) and zone-boundary points as defined for a simple orthorhombic system.

We find two SiC bi-layers to be affected in energy (Fig. 3), but the reconstruction alone cannot explain the stabilisation of the equilibrium structures (Table 1), since although there is clearly a stronger reconstruction in the uppermost layer, the second layer involves a reconstructed bond which is marginally longer than the bulk counterpart. We have therefore examined the impact of the vacancy location upon the geometry at the interface. In particular, Table 2 lists the results of a statistical analysis of the locations of the silicon atoms adjacent to the first oxygen layer. For each site we have determined the displacement in the [0001]-direction relative to the location of the comparable atom in the defect-free slab. For V_C^1 the deformation represented by the tabulated data is consistent with the immediate proximity of the vacancy and three of the silicon atoms analysed are involved in the reconstruction. It is therefore unsurprising that there are displacements in both the [0001] and [000$\bar{1}$] directions, ranging over only slightly less than 1 Å.

The data for V_C^2 are smaller than for V_C^1, but significantly greater than for V_C^3, so that despite the relatively less favourable reconstruction indicated in Table 1 for the second layer, the relaxation at the interface provides a stabilising effect resulting in a lower energy than layer 3. Diffusion in the third carbon layer is between h-sites (hh), and we find an activation energy profile that closely resembles that obtained for the hh process in bulk 4H-SiC. The implication is that lateral diffusion (hh and kk) more than two SiC by-layers from the SiO_2 interface can be considered to be effectively bulk-like.

Table 2: Range and standard deviation (SD) of [0001] displacements of Si atoms in the SiC bonded to oxygen in the SiO_2 as a function of the location of the vacancy, all values in Å.

Defect	Range	SD(z)
V_C^1	0.840	0.161
V_C^2	0.213	0.053
V_C^3	0.084	0.026

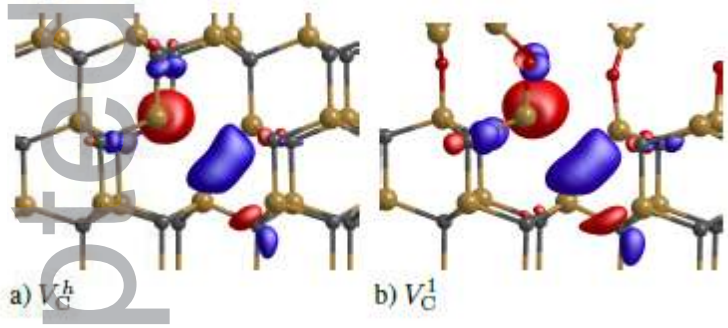

Figure 5: Illustrative wave function isosurfaces for the highest occupied bands of V_C^h and V_C^1 (Fig. 4). Red and blue isosurfaces represent positive and negative wave function components, respectively. Yellow, grey and red atoms are Si, C and O, respectively. The horizontal direction is approximately along [1 $\bar{1}$ 00], and the vertically upward direction is [0001].

Further evidence for the impact of relaxation of the equilibrium structures close to the interface is seen in the electronic structure. The two Si-Si reconstructions result in a single occupied state (Fig. 4 a, b, c, e and f) derived from a significant splitting of the approximately three-fold-degenerate state of the unreconstructed case (Fig. 4d). This occupied gap-state is dominated by an anti-bonding combination of orbitals from the two Si–Si covalent reconstructed bonds, as illustrated in Fig. 5. Indeed, all fully relaxed cases examined for this study show qualitatively similar wave functions and band structures. Quantitatively, however, there are key differences. Comparing the band structures of V_C^h and V_C^1 shows that the highest occupied band is closer to the valence band for the vacancy at the interface, consistent with the strengthening of the reconstructed bonds. However, the locations of the occupied band for V_C^k and V_C^2 are very similar, consistent with the structural analysis above, reinforcing the role of the interfacial

relaxation in stabilisation of V_C in the second layer.

We next turn to the increase in energy for the transition state structure, and we focus our attention upon the *hh*-process associated with our model diffusion in the first layer.

The transition state structure is illustrated in Fig. 6. It is characterised by the moving carbon atom lying midway between two carbon sites and being bonded to three Si atoms. One of these three Si-neighbours is three-fold-co-ordinated (the Si atom to which the C atom is bonded throughout the process). The other two Si neighbours are fully-co-ordindated, and are Si-sites adjacent to the two different C-sites involved in the diffusion process. There are a number of pairs of Si atoms that could reconstruct based upon proximity, and these are indicated in the figure by the translucent bonds.

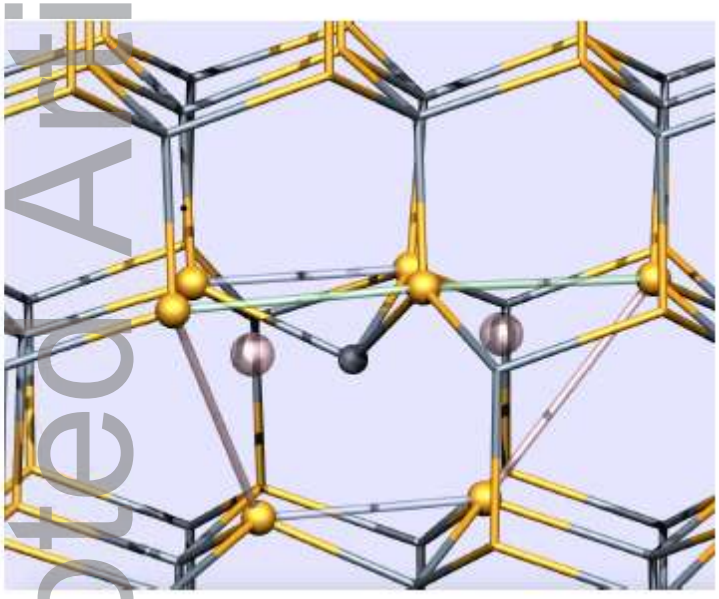

Figure 6: Schematic representation of the saddle point structure of V_C^h. The yellow and grey sites are Si and C, respectively, with the translucent spheres indicating the carbon sites between which the C atom is moving. Si sites indicated with spheres are those adjacent to the vacancy at either end of the process. Possible reconstructions are shown as translucent bonds. The structure is shown with the vertical and horizontal slightly offset from [0001] and [1 $\bar{1}$ 00] to facilitate views of atoms in the background.

The three Si-C bonds indicated as solid at the centre of the structure in Fig. 6 are slightly shorter for V_C^1 than for V_C^h, which may reflect the relatively easier relaxation of the SiO_2 noted for the equilibrium structure. Although based upon inter-nuclear distances there is no clear evidence of Si-Si reconstruction at the edges of the structure (the translucent bonds approximately along the *c*-axis in Fig. 6), two Si-Si distances are significantly shorter than the 3.06 Å bulk-reference. These are indicated as blue translucent bonds in Fig. 6, and are the same or shorter for V_C^1 than for V_C^h. Indeed, generally we found for clearly identified chemical bonds in the V_C^1 and V_C^h transition state structures, the inter-nuclear distances are shorter at the interface than in

bulk. On this basis one might expect the interfacial transition state to be more energetically favourable than the bulk case, in contrast to the calculated energies (Fig. 3).

However, the electronic structure (not shown) provides key additional evidence. In the case of the transition state structure in bulk 4H-SiC there is one occupied state in the band-gap, similar to the equilibrium case. For the transition state structure the occupied gap state is largely associated with bonding combinations of orbitals representing weak reconstructions between the three-fold-co-ordinated Si atom indicated in green in Fig. 6. In contrast, for V_C^1 there are *two* occupied levels in the band-gap, with the additional level associated with weak reconstructions between the atoms at the ends of the structure, indicated by the reconstructions approximately along the c-axis in the figure. This state is about 0.2 eV above the valence band top.

Our interpretation of our energy and structure data is therefore as follows. Although the more flexible environment at the interface allows for relaxation and stronger bonding adjacent to the moving carbon atom, this destabilises a larger number of weaker Si–Si reconstruction interactions across the whole structure. This pushes up the energy of the electrons associated with these reconstructions, and the net effect is an increase in the total energy: the energy saved by the relaxation of the core of the transition state structure is outweighed by costs elsewhere in the system.

4 Summary

We have presented an investigation into stabilisation and diffusion processes of V_C within SiC in the immediate vicinity of a SiO_2/(0001)-4H-SiC interface by means of density functional calculations. We find that V_C can form stronger Si–Si reconstruction bonds in the interfacial layer and a lowering of the energy of band-gap states, which correlate with a lowering in the formation energy of the defect in this site. However, stabilisation of the vacancy more distant from the interface is not driven by the same process, but rather proximity to the interfaces allows for greater interfacial relaxation where the vacancy is close-by. Our findings also suggest that if the vacancy lies more than two SiC bi-layers from the interface, its behaviour differs insignificantly from its bulk counterpart. For diffusion, the interfacial layer has a higher activation energy due to the stabilisation of the vacancy and an increased energy of the transition state linked to the destabilisation of reconstructions, reducing the rate at which the vacancy is expected to migrate in the vicinity of the interface.

Finally, we note that the findings of higher barriers and stabilisation of vacancies at the SiO_2/4H-SiC interface are consistent with a high density of trap in this region observed in experimental [26].

Acknowledgements This research made use of the High Performance Computing service at Newcastle University. HA thanks the Omm Al-Qura University (KSA) for sponsoring her PhD study.

References

[1] K. Kawahara, X. T. Trinh, N. .T. Son, Nguyen, E. Janzén, J. Suda and T. Kimoto,

Appl. Phys. Lett **102**, 112106 (2013).

[2] K. Kawahara, J. Suda, T. Kimoto, J. Appl. Phys. **111**, 5, 053710 (2012).

[3] C. J. Kirkham and T. Ono, J. Phys. Soc. of Japan **85**, 024701 (2016).

[4] T. Kimoto, K. Danno, and J. Suda, Physica Status Solidi B **245**,1327–1336 (2008).

[5] Z. Q. Fang, D. C. Look, A. Saxler and W. C. Mitchel, Physica B, **308** 706–709 (2001).

[6] T. Hornos, A. Gali, and B. G. Svensson, Mater. Sci. Forum **11**, 261–264 (2011).

[7] P. R. Briddon and R. Jones, Physica Status Solidi B **131**,131-171 (2000).

[8] H. Alsnani, J. P. Goss, S. H. Olsen, M. J. Rayson, P. R. Briddon and A. B. Horsfall in 12th European Conference on Silicon Carbide Related Materials (ECSCRM-2018), Birmingham, UK, September (2018).

[9] J. P. Perdew and Y. Wang, Phys. Rev. B **45**, 13244 -13249 (1992).

[10] J. P. Goss, M. J. Shaw, and P. R. Briddon, in *Theory of Defects in Semiconductors*, Vol. 104 of *Topics in Applied Physics*, edited by David A. Drabold and Stefan K. Estreicher (Springer, Berlin/Heidelberg, 2007), pp. 69–94.

[11] J. Rozen, S. Dhar, S. T. Pantelides, L. C. Feldman, S. Wang, J. R. Williams, and V. V. Afanas'ev, Appl. Phys. Lett/ **91**, 153503 (2007).

[12] M. J. Rayson and P. R. Briddon, Phys. Rev. B **20**, 205104, (2009).

[13] H. J. Monkhorst and J. D. Pack, Phys. Rev. B **12**, 5188–5192, (1976).

[14] G. Henkelman, B. P. Uberuaga and H. Jónsson, J. Chem. Phys. **113**, 9901 (2000); G. Henkelman and H. Jónsson, J. Chem. Phys. **113**, 9978 (2000).

[15] J. Isoya, T. Umeda, N. Mizuochi, T. Son, E. Janzén and T. Ohshima, Physica Status Solidi B, **245**(7), 1298–1314 (2008).

[16] L. Gordon, A. Janotti and C. G. Van De Walle, Phys. Rev. B **92**, 045208 (2015).

[17] L. Torpo, T. E. Staab and R. M. Nieminen, Phys. Rev. B **65**, 085202 (2002).

[18] F. Bechstedt, P. Käckell, A. Zywietz, K. Karch, B. Adolph, K. Tenelsen and J. Furthmüller, Physica Status Solidi B,**202**, 35–62 (1997).

[19] J. M. Knaup, P. Deák, T. Frauenheim, A. Gali, Z. Hajnal and W. J. Choyke, Phys. Rev. B **11**, 115323 (2005).

[20] M. Bockstedte, M. Heid, and O. Pankratov, Phys. Rev. B **67**, 193102 (2003).

[21] T. Umeda, J. Isoya, N. Morishita, T. Ohshima and T. Kamiya, Phys. Rev. B, **69**, 12, 121201 (2004).

[22] F. Devynck, F. Giustino, P. Broqvist, and A. Pasquarello, Phys. Rev. B **76**, 075351 (2007).

[23] P. Deák, J. M. Knaup, T. Hornos, C. Thill, A. Gali and T. J. Frauenheim, Appl. Phys. D **40**, 6242 (2007).

[24] A. Gali, Physica Status Solidi B **248**, 1337–1346 (2001).

[25] T. Umeda, J. Isoya, N. Morishita, T. Ohshima, E. Janzén and A. Gali, Phys. Rev. B **97**, 115211 (2009).

[26] T. Zheleva, A. Lelis, G. Duscher, F. Liu, I. Levin and M. Das, Appl. Phys. Lett. **93**, 022108 (2008).

GTOC image:

The majority of electronically active defects in SiC are located deep within the bandgap, thereby degrading the carrier transport properties of SiC. This study compares of diffusion of a carbon vacancy in different (0001)-layers relative to a SiO_2/SiC interface using the density functional theory simulations. The result shows that vacancies in the upper layers are stabilised due to stronger bonding and interfacial relaxation.